Structural Investigation of the Antibiotic and ATP-Binding Sites in Kanamycin Nucleotidyltransferase[†,‡]

Lars C. Pedersen, Matthew M. Benning, and Hazel M. Holden*

Institute for Enzyme Research, Graduate School, and Department of Biochemistry, University of Wisconsin, Madison, Wisconsin 53705

Received June 28, 1995; Revised Manuscript Received July 27, 1995[⊗]

ABSTRACT: Kanamycin nucleotidyltransferase (KNTase) is a plasmid-coded enzyme responsible for some types of bacterial resistance to aminoglycosides. The enzyme deactivates various antibiotics by transferring a nucleoside monophosphate group from ATP to the 4′-hydroxyl group of the drug. Detailed knowledge of the interactions between the protein and the substrates may lead to the design of aminoglycosides less susceptible to bacterial deactivation. Here we describe the structure of KNTase complexed with both the nonhydrolyzable nucleotide analog AMPCPP and kanamycin. Crystals employed in the investigation were grown from poly(ethylene glycol) solutions and belonged to the space group $P2_12_12_1$ with unit cell dimensions of a = 57.3 Å, b = 102.2 Å, c = 101.8 Å, and one dimer in the asymmetric unit. Least-squares refinement of the model at 2.5 Å resolution reduced the crystallographic R factor to 16.8%. The binding pockets for both the nucleotide and the antibiotic are extensively exposed to the solvent and are composed of amino acid residues contributed by both subunits in the dimer. There are few specific interactions between the protein and the adenine ring of the nucleotide; rather the AMPCPP molecule is locked into position by extensive hydrogen bonding between the α-, β-, and γ-phosphates and protein side chains. This, in part, may explain the observation that the enzyme can utilize other nucleotides such as GTP and UTP. The 4′-hydroxyl group of the antibiotic is approximately 5 Å from the α-phosphorus of the nucleotide and is in the proper orientation for a single in-line displacement attack at the phosphorus. Glu 145, which lies within hydrogen-bonding distance of the 4′-hydroxyl group, is proposed to be the active site base.

Aminoglycoside antibiotics consist of amino sugars linked to an aminocyclitol moiety through glycosidic bonds as shown in Figure 1. The bactericidal effect of these compounds is believed to occur through their irreversible binding to the bacterial ribosomes (Moellering, 1983). Although there are newer, less toxic compounds on the market, the aminoglycosides still play useful roles in the treatment of serious infections caused by a broad range of microorganisms (Edson & Terrel, 1991; Johnson & Hardin, 1992). Unfortunately, due to past widespread usage of these antibiotics in clinical settings, bacterial strains have emerged that render these compounds ineffective. Resistance to aminoglycosides is typically conferred by the enzymatic activity of plasmid-coded acetyltransferases, phosphotransferases, and nucleotidyltransferases [for a review, see Shaw *et al.* (1993)]. Kanamycin nucleotidyltransferase (KNTase) is one such enzyme and catalyzes the transfer of a nucleoside monophosphate group from a nucleotide to the 4′-hydroxyl group of kanamycin. First isolated from *Staphylococcus aureus*, the enzyme can utilize ATP, GTP, or UTP as the nucleoside monophosphate donor and is capable of deactivating a number of different aminoglycosides (Le Goffic *et al.*, 1976a,b; Davies & Smith, 1978).

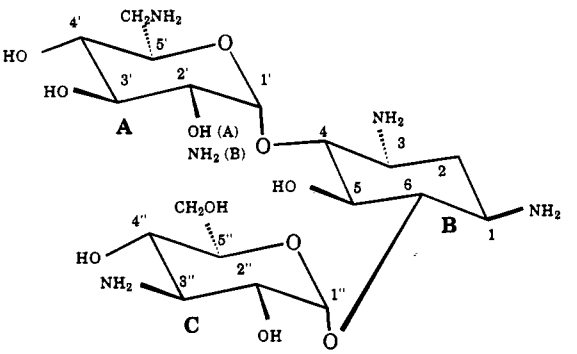

FIGURE 1: General structure of the antibiotic kanamycin. Kanamycins A and B differ only at the 2′-position as indicated. Both the 4′- and the 4″-hydroxyl groups are susceptible to nucleotidylation by KNTase.

The three-dimensional structure of KNTase was recently determined by X-ray crystallographic techniques (Sakon *et al.*, 1993). From this structural study it was shown that the enzyme was dimeric rather than monomeric as originally believed (Sadaie *et al.*, 1980). The individual subunits of KNTase are remarkably extended as shown in Figure 2a and can be described in terms of two structural domains. The N-terminal domain, delineated by Met 1 to Glu 127, is characterized by a five-stranded mixed β-pleated sheet whereas the C-terminal motif, formed by Ala 128 to Phe 253, contains five α-helices, four of which form an up-and-down α-helical bundle. As can be seen in Figure 2b, the two subunits interact extensively by wrapping around one another to form a rather large cavity which can easily accommodate a variety of aminoglycosides. On the basis

[†] This research was supported in part by a grant from the NIH (DK47814).

[‡] X-ray coordinates have been deposited with the Brookhaven Protein Data Bank under the filename 1KNY.

* To whom correspondence should be addressed.

[⊗] Abstract published in *Advance ACS Abstracts,* October 1, 1995.

0006-2960/95/0434-13305$09.00/0

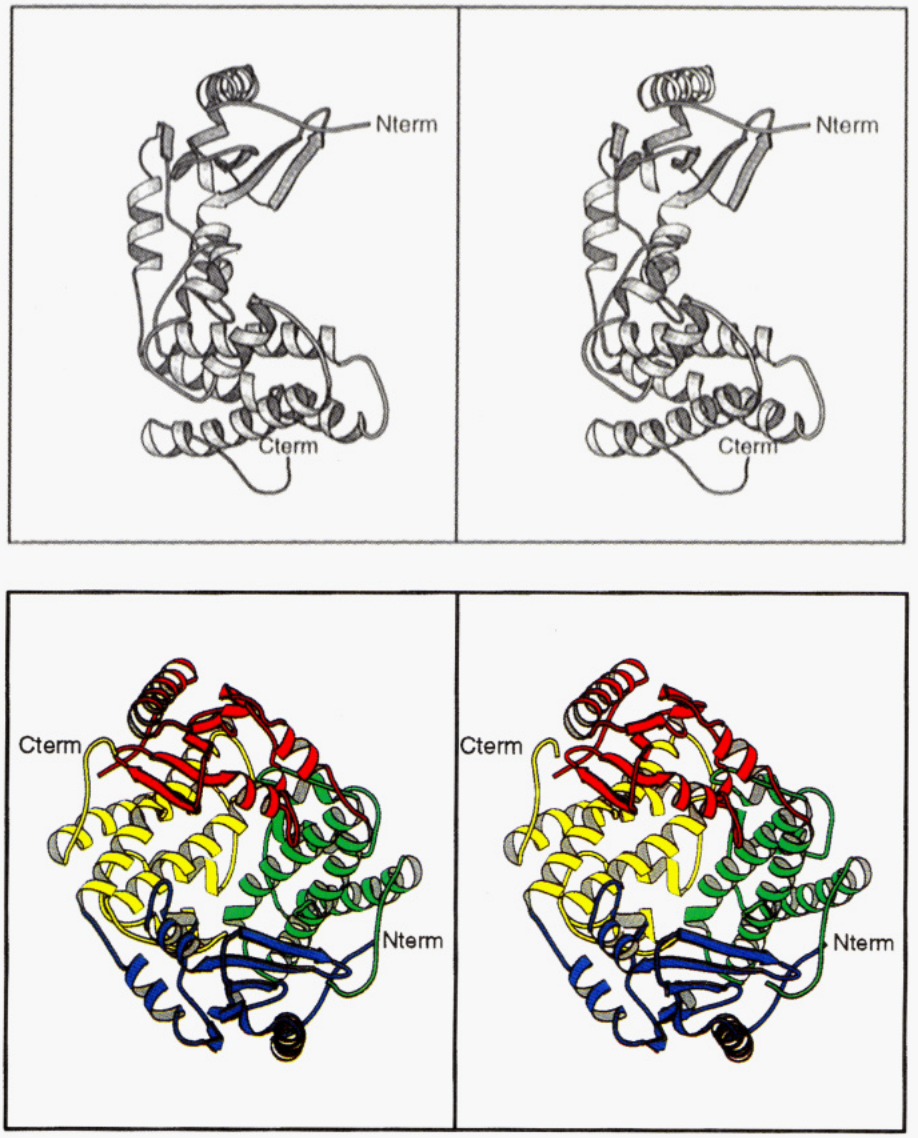

FIGURE 2: Ribbon representation of the apo form of KNTase. Models for the individual monomer and the dimer of KNTase are shown in panels a (top) and b (bottom), respectively. The domains depicted in blue and yellow belong to subunit I; those in red and green represent subunit II. This figure was prepared with the software package MOLSCRIPT (Kraulis, 1991).

of this initial structural investigation, the two active sites for the KNTase homodimer were tentatively located and shown to be formed by both subunits (Sakon *et al.*, 1993).

Here we describe the three-dimensional structure of KNTase complexed with AMPCPP, a nonhydrolyzable analog of ATP, and kanamycin. This structural investigation provides a more complete description of the active site of this enzyme and reveals both important protein−nucleotide and protein−antibiotic interactions. Detailed structural information concerning the active site of KNTase may ultimately lead to the design of new and more effective aminoglycosides and possibly to the production of KNTase inhibitors. This is especially important in light of both the alarming and rapid increase in the emergence of antibiotic-resistant bacterial strains and the lack of significant new antibiotics appearing on the pharmaceutical market.

MATERIALS AND METHODS

Purification and Crystallization Procedures. The KNTase mutant, D80Y, was expressed in the *Escherichia coli* overproducing strain BL21(DE3) carrying the expression plasmid pX(T7)TK1 (Studier & Moffatt, 1986; Liao, 1991). These cells were stored at −70 °C prior to use. The enzyme purification scheme employed was a modification of previously reported procedures and included an initial chromatographic step with a DEAE-Sephadex-6505 column followed by a TSK phenyl-5PW hydrophobic column and subsequent use of an HPLC Mono-Q HR10/10 column (Liao *et al.*, 1986; Liao, 1991; Sadie *et al.*, 1980; Sakon *et al.*, 1993). The purified protein was stored in 10 mM Tris-HCl, pH 7.5 at −20 °C. Thus far it has not been possible to obtain X-ray quality crystals for the wild-type enzyme.

Prior to crystallization, the protein, at 15 mg/ml, was incubated with 10 mM kanamycin A for 1 h at 4 °C. X-ray diffraction quality crystals were obtained by the hanging drop method of vapor diffusion. For such experiments, 5 μL of the protein−kanamycin solution was mixed on silanized coverslips with 5 μL of a solution containing 12.5% PEG 3350, 150 mM $MgCl_2$, 5 mM NaN_3, and 100 mM Hepes (pH 7.7). These droplets were equilibrated against the 12.5% PEG solution. Crystals generally appeared within 1 week with some achieving maximum dimensions of 0.3 mm × 0.3 mm × 0.7 mm.

Table 1: Intensity Statistics for the Native X-ray Data

native	resolution range (Å)								
	overall	100.00−5.00	3.97	3.47	3.15	2.92	2.75	2.61	2.50
no. of measurements	51522	7655	7898	7331	6580	5992	5708	5299	5059
no. of independent reflections	20767	2513	2548	2590	2600	2611	2641	2626	2638
completeness of data (%)	81	84	89	90	88	83	76	70	65
av intensity	4571	9095	10 000	5980	3266	1673	976	666	487
av σ	438	366	499	473	443	424	421	429	442
R factor[a] (%)	5.0	3.5	3.4	4.5	6.8	11.1	17.0	21.9	29.1

[a] R factor = $(\Sigma|I - \bar{I}|/\Sigma I) \times 100$.

Prior to X-ray data collection, the crystals were transferred to a solution containing 14% PEG 3350, 150 mM $MgCl_2$, 5 mM NaN_3, 100 mM Hepes (pH 7.7), 20 mM kanamycin A, and 5 mM adenosine 5′-α,β-methylenetriphosphate (AMPCPP). To minimize crystal cracking, the concentration of AMPCPP was slowly increased to 10 mM and finally to 16 mM over a period of 2 h. Crystals were soaked in this kanamycin−AMPCPP solution for 24 h. On the basis of precession photography, the crystals were shown to belong to the space group $P2_12_12_1$ with unit cell dimensions of a = 57.3 Å, b = 102.2 Å, c = 101.8 Å, and one dimer in the asymmetric unit.

X-ray Data Collection and Processing. X-ray diffraction data were collected to 2.5 Å resolution at 4 °C with a Siemens X1000D area detector system equipped with double-focusing mirrors. The X-ray source was Cu Kα radiation from a Rigaku RU200 rotating anode generator operated at 50 kV and 50 mA. These X-ray data were subsequently processed and scaled with the software packages XDS and XSCALIBRE, respectively (Kabsch, 1988a,b; Wesenberg and Rayment, unpublished results). Relevant X-ray data collection statistics may be found in Table 1.

Computational Methods. The structure of the KNTase−kanamycin−AMPCPP complex was solved by the technique of molecular replacement with the software package AMORE (Navaza, 1987). The structure of the double mutant D80Y T130K, previously solved to 3.0 Å resolution, served as the search model (Sakon *et al.*, 1993). The rotational and translational searches were conducted with X-ray data between 8.0 and 3.5 Å. A solution corresponding to the dimer in the asymmetric unit was obtained and was as follows: $\alpha = 8.69°$, $\beta = 158.16°$, $\gamma = 108.34°$, $a = 0.4535$, $b = 0.0696$, and $c = 0.0172$. Following rigid body refinement, the R factor was reduced to 33.9% for all measured X-ray data between 20.0 and 3.5 Å.

The three-dimensional model was subsequently refined by multiple cycles of manual model building with the program FRODO and least-squares refinement with the software package TNT (Jones, 1985; Tronrud *et al.*, 1987). Ideal stereochemistry employed for the kanamycin substrate was based on the small molecule structural determination of Koyama *et al.* (1968). X-ray coordinates for AMPCPP were derived from the crystal structure of ATP (Kennard *et al.*, 1971). In addition to the protein atoms, the model contained 44 water molecules, 2 magnesium ions, 2 AMPCPP molecules, and 2 kanamycin antibiotics. The average temperature factors for the polypeptide chain backbone atoms were 29.9 and 34.8Å^2, respectively, for subunits I and II. Backbone atoms for the two subunits in the dimer superimpose with a root-mean-square deviation of 0.44 Å. Relevant refinement statistics may be found in Table 2.

Table 2: Least-Squares Refinement Statistics

resolution limits (Å)	30.0−2.5
R factor[a] (%)[a]	16.8
no. of reflections used	19 405
no. of protein atoms	4187
no. of solvent atoms	46
weighted rms deviations from ideality	
bond length (Å)	0.014
bond angle (deg)	2.5
planarity (trigonal) (Å)	0.006
planarity (other planes) (Å)	0.012
torsional angle[b] (deg)	19.2

[a] R factor = $\Sigma|F_o - F_c|/\Sigma|F_o|$, where F_o is the observed structure factor amplitude and F_c is the calculated structure factor amplitude. [b] The torsional angles were not restrained during the refinement.

RESULTS AND DISCUSSION

The original model of KNTase was derived from crystals of a thermostable double mutant, D80Y and T130K (Sakon *et al.*, 1993). While these crystals allowed for the tracing of the polypeptide chain, their limited resolution of approximately 3 Å hindered further structural investigations. The model of KNTase presented here is based on X-ray diffraction data from crystals of the site-directed mutant D80Y. These crystals diffract beyond 2.5 Å. An α-carbon trace of the new KNTase model is displayed in Figure 3. The α-carbon positions for the original model and the KNTase structure presented here superimpose with a root-mean-square deviation of 0.75 Å. Due to the increase in resolution of the X-ray data, however, it is now possible to define the secondary structure of KNTase in more detail.

The individual subunits of the dimer are divided into two structural domains of approximately equal size. The main structural motif of the N-terminal domain is a five-stranded, predominantly antiparallel, β-sheet formed by Val 31 to Tyr 37, Asp 50 to Met 57, Glu 63 to Thr 69, Trp 73 to Ser 81, and Leu 107 to Asp 111. The two β-strands delineated by Asp 50 to Met 57 and Trp 73 to Ser 81 run parallel to one another. The N-terminal domain is also characterized by five α-helices formed by Arg 9 to Lys 26, Ser 39 to Arg 42, Glu 82 to Ala 89, Pro 97 to Gln 102, and Tyr 115 to Lys 124. In addition to these major secondary structural elements, the N-terminal domain contains four well-defined reverse turns as follows: two type I (Gly 46 to Ser 49 and Glu 93 to Trp 96), one type II (Thr 59 to Ala 62), and one type II′ (Tyr 27 to Asp 30). The C-terminal domain contains two long α-helices delineated by Ala 128 to Val 155 and Leu 162 to His 180 and three smaller α-helices formed by Val 191 to Ala 195, Asp 206 to Ser 214, and Ser 220 to His 241. The second and third α-helices in the C-terminal domain are connected by a type I turn (Thr 187 to Ser 190). A type II turn formed by Pro 202 to Tyr 205 serves as a

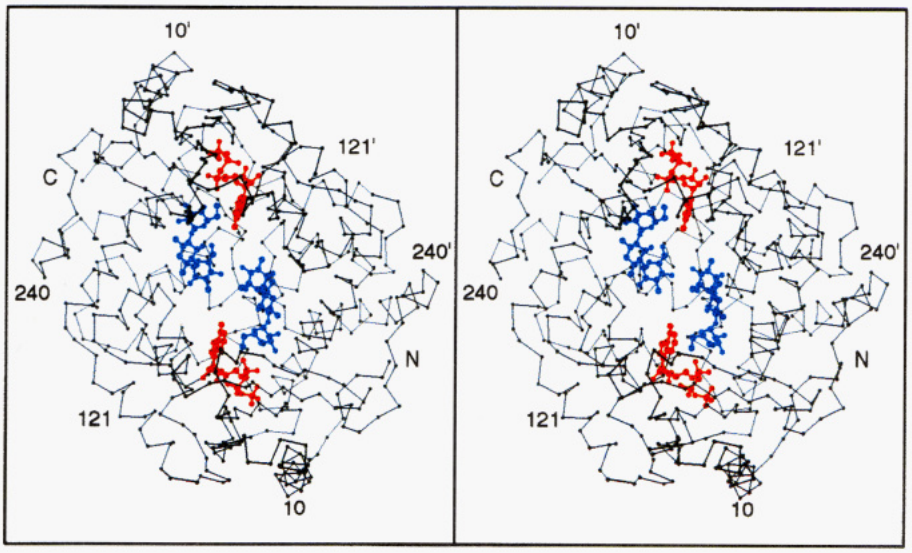

FIGURE 3: α-Carbon trace of the KNTase dimer with bound substrates and nucleotide analogs. The quaternary structure of the enzyme is such that approximately 6000 Å^2 of surface area is buried upon dimerization as calculated according to the method of Lee and Richards (1971) with a probe sphere of 1.4 Å. The nucleotides and antibiotics are depicted in red and blue bonds, respectively. As can be seen, the β- and γ-phosphates of the nucleotides are the most buried with the antibiotics sitting at the surface of the large cavity formed by the two subunits. The positions of several amino acid residues are indicated to aid the reader in following the course of the polypeptide chain. The primed numbers refer to the second subunit in the dimer.

link between the third and fourth α-helices. In the original KNTase model, the surface loops defined by Tyr 27 to Asp 30, Arg 42 to Gly 46, and Glu 60 to Ala 62 were disordered in the electron density map. These residues are clearly defined in the present model.

In the original structure determination of KNTase, there were two large peaks of electron density that were symmetry-related to one another and were positioned between Glu 76 (subunit I) and Glu 145 (subunit II) and between Glu 76 (subunit II) and Glu 145 (subunit I), respectively. Preliminary atomic absorption experiments indicated that KNTase binds Zn^{2+} ions, and as such these peaks were modeled as cations (Sakon *et al.*, 1993). In the electron density map employed for this structural investigation, however, these peaks of high electron density are not present, thereby suggesting that the binding of the cations to KNTase may have been simply the result of the original crystallization conditions which included 3 mM $CoCl_2$. One final difference between the two models involves Pro 158. The new electron density map calculated to 2.5 Å resolution clearly shows that this residue adopts a cis conformation in both subunits.

Difference electron density corresponding to the nucleotides and the antibiotics is displayed in Figure 4. As can be seen, the electron densities for the AMPCPP molecules are well ordered. Given the fact that KNTase can deactivate a variety of aminoglycosides and can modify both the 4′- and the 4″-hydroxyl groups of kanamycin (Schwotzer *et al.*, 1978), it is not surprising that the electron densities corresponding to the antibiotics are less clear as can be seen in Figure 4. For the present study, the antibiotics have been fitted into the electron density map such that their 4′-hydroxyl groups are close to the AMPCPP moieties.

A close-up stereoview of the active site for KNTase is given in Figure 5a, and a schematic of the protein−substrate interactions is shown in Figure 5b. In the KNTase dimer the two nucleotides are approximately 17 Å apart while the closest approach between the two kanamycin molecules is 3.5 Å. The nucleotide binding pocket is exposed to the solvent and composed of amino acid residues contributed by both subunits. Those residues located within approximately 5.0 Å of the nucleotide include Tyr 37 to Ser 39, Arg 42, Thr 44 to Gly 46, Ser 49, Asp 50, Glu 52, Tyr 88, Asp 95, Leu 98 to Gln 102, and Tyr 185 to Ser 188 from subunit I and Glu 145, Lys 149, and Asn 152 from subunit II. The adenine portion of the nucleotide is involved in few specific interactions with the protein and thus may explain why ATP, GTP, and UTP are all substrates for the enzyme. Likewise, only one of the hydroxyl groups of the ribose, namely, O3R, lies within 3.0 Å of $N^{\eta 2}$ of Arg 42 (subunit I). The majority of the nucleotide−protein interactions involve the phosphoryl oxygens and various side-chain moieties. Specifically, the α-phosphoryl oxygens are within 3.2 Å of Asp 50 and Glu 52 from subunit I, Glu 145 and Lys 149 from subunit II, and a well-ordered water molecule, the β-phosphoryl oxygens lie within 3.0 Å of Arg 42 and Thr 187 from subunit I, and the γ-phosphoryl oxygens interact with Ser 39 and Ser 49 from subunit I. In addition, the backbone amide nitrogen of Ser 39 is in the proper orientation for hydrogen bonding to one of the β-phosphoryl oxygens. There is a magnesium ion coordinated by the β- and γ-phosphates of the AMPCPP and the carboxylate group of Glu 52. The Mg^{2+}−AMPCPP complex is in the Δ-screw sense configuration.

In the apoenzyme structure there was a ring of seven negatively charged amino acid residues, Glu 52, Glu 67, Glu 76, and Asp 50 from subunit I and Glu 141, Glu 142, and Glu 145 from subunit II, that were postulated to form a portion of the antibiotic binding site (Sakon *et al.*, 1993). Indeed, many of these residues interact with the positively charged antibiotic. The amino sugar labeled A in Figure 1 interacts most extensively with the enzyme and is wedged against the adenine ring of the AMPCPP. This portion of the aminoglycoside participates in hydrogen-bonding interactions with the side chains of Glu 67, Glu 76, and Lys 74 from subunit I and Glu 141 and Glu 145 from subunit II. The aminocyclitol moiety, labeled B in Figure 1, lies near the side chains of Ser 94 and Glu 141 from subunit II. The third sugar has few specific interactions with the protein.

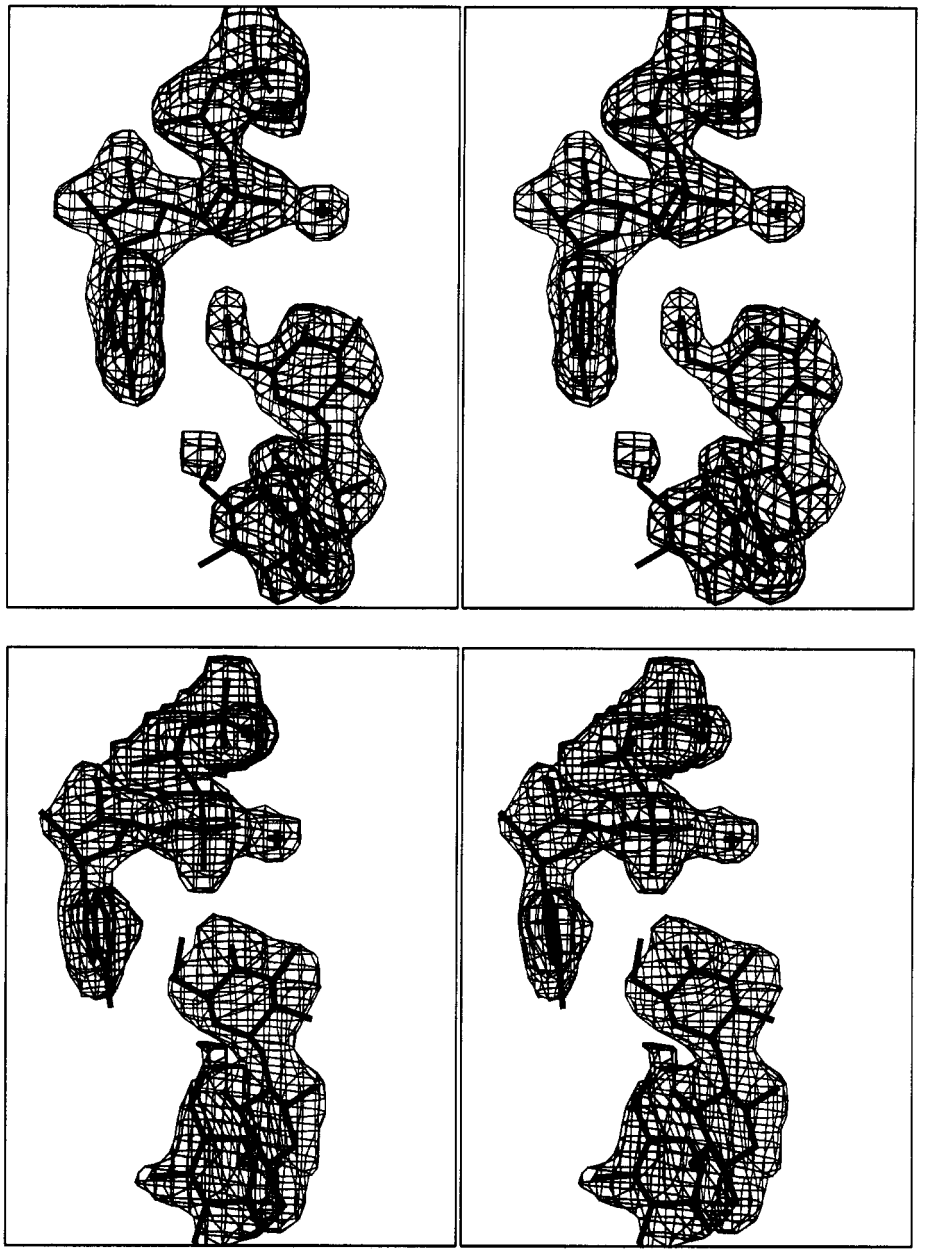

FIGURE 4: Difference electron density observed for the nucleotide and kanamycin. The map sections shown were calculated with coefficients of the form $(F_o - F_c)$, where F_o was the native structure factor amplitude and F_c was the calculated structure factor amplitude from the model lacking the coordinates for the antibiotics, the nucleotides, and the magnesium ions. The electron density map was calculated to 2.5 Å resolution and contoured at 2.5σ. Map sections shown in (a, top) and (b, bottom) correspond to subunits I and II, respectively. The magnesium ions, coordinated by the β- and γ-phosphates, are indicated by crosses in (a) and (b). In addition to the magnesiums, there are water molecules, also depicted as crosses, lying within hydrogen-bonding distances of the α-phosphoryl oxygens.

Due to the internal symmetry that exists within the kanamycin molecule itself, the difference electron density does not rule out the possibility that the 4″-hydroxyl group may be pointing toward the α-phosphorus.

A model for the enzymatic mechanism of KNTase has not been biochemically investigated thus far. The enzyme, aminoglycoside nucleotidyltransferase 2″-I, however, has been extensively studied (Gates & Northrop, 1988a). Like KNTase, this enzyme transfers a nucleoside monophosphate group from a nucleotide to a hydroxyl group of an aminoglycoside. From the research of Gates and Northrop (1988b,c), it has been established that aminoglycoside nucleotidyltransferase 2″-I obeys the Theorell-Chance kinetic mechanism in which nucleotide binding to the enzyme is followed by aminoglycoside binding. In addition, it has been demonstrated that pyrophosphate is released followed by the nucleotidyl aminoglycoside and that the rate-limiting step is product release. Further studies by Van Pelt *et al.* (1986) have indicated that the nucleoside monophosphate is directly transferred to the hydroxyl group of the antibiotic without an intermediate step and that the reaction proceeds through inversion of the stereochemistry about the α-phosphorus.

Based on the structure of the KNTase−AMPCPP−antibiotic complex described here, it is possible to propose a catalytic mechanism for the enzyme. As can be seen in Figure 6, the 4′-hydroxyl group of the antibiotic is situated approximately 5.0 Å from the α-phosphate of the nucleotide. In turn, the carboxylate group of Glu 145 from subunit II is located within hydrogen-bonding distance to this hydroxyl group. According to the proposed mechanism, Glu 145 acts as the general base that abstracts the proton from the 4′-hydroxyl group, thereby activating the kanamycin for the

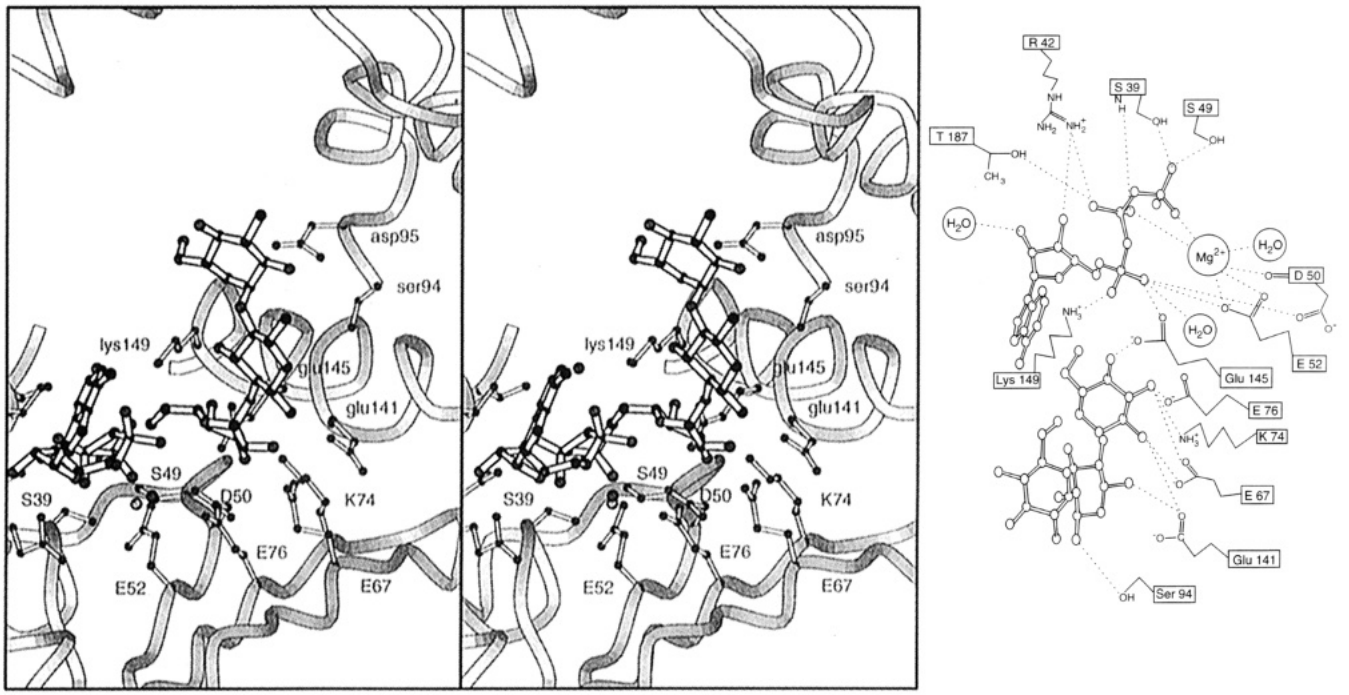

FIGURE 5: KNTase active site. (a, left) Those amino acid residues contributed by subunits I and II are labeled according to the one-letter and three-letter codes, respectively. For the sake of clarity, only those amino acid residues that lie within approximately 3.5 Å of the substrates and that can participate in hydrogen bonding are displayed. (b, right) Possible interactions between the protein and the substrates, within 3.2 Å, are indicated by dashed lines.

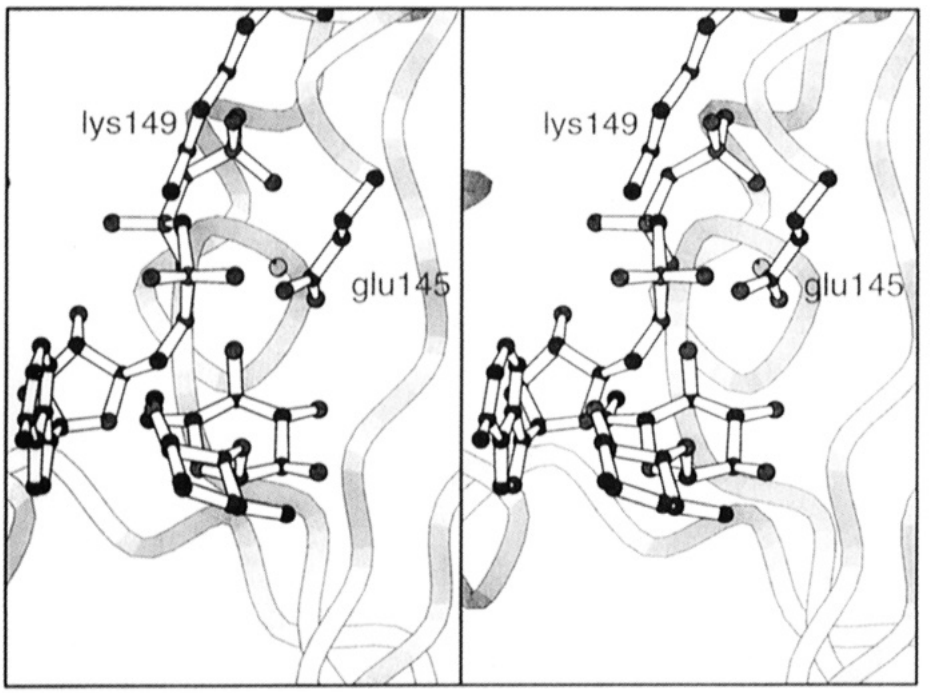

FIGURE 6: Stereoview of the amino acid residues thought to be important in catalysis. The figure is centered around the 4′-hydroxyl group of kanamycin that is nucleotidylated by KNTase. Only a portion of the antibiotic is shown. Glu 145 is thought to be the active site base. The magnesium ion, coordinated by the β- and γ-phosphates, is depicted as an open sphere.

subsequent attack at the α-phosphorus of the nucleotide. Both the nucleotide and the antibiotic are in the proper orientation for a single in-line displacement reaction. The Mg^{2+}–pyrophosphate moiety would serve as an excellent leaving group. In addition, the close proximity of Lys 149 to one of the α-phosphoryl oxygens could increase the electrophilic character of the phosphorus center, thus making it more susceptible to nucleophilic attack. While the distance between the 4′-hydroxyl group and the α-phosphorus is 5.0 Å, the enzyme may undergo a conformational change during catalysis to decrease this distance. Furthermore, the structure described here is that complexed with a nucleotide analog. Slight conformational differences due to the replacement of a methylene group for a bridging oxygen could also account for this longer than expected distance between the nucleotide and the antibiotic. Attempts to grow crystals in the presence of Lu^{3+}ATP, an inhibitory analog of Mg^{2+}ATP, are in progress (Morrison & Cleland, 1983). The putative reaction

mechanism of KNTase presented here may possibly serve as a model for the more complex polymerases that catalyze nucleotidyl phosphate transfer. Experiments to confirm the proposed mechanism are presently underway.

ACKNOWLEDGMENT

The authors thank Dr. W. W. Cleland for suggesting the catalytic mechanism and for critically reading the manuscript and Dr. Gary Wesenberg for help in the preparation of the figures. The technical expertise of Robert Smith is gratefully acknowledged.

REFERENCES

Davies, J., & Smith, D. I. (1978) *Annu Rev. Microbiol. 32*, 469–518.

Edson, R. S., & Terrell, C. L. (1991) *Mayo Clin. Proc. 66*, 1158–1164.

Gates, C. A., & Northrop, D. B. (1988a) *Biochemistry 27*, 3820–3825.

Gates, C. A., & Northrop, D. B. (1988b) *Biochemistry 27*, 3826–3833.

Gates, C. A., & Northrop, D. B. (1988c) *Biochemistry 27*, 3834–3842.

Johnson, J. G., & Hardin, T. C. (1992) *Clin. Podiatr. Med. Surg. 9*, 443–464.

Jones, A. T. (1985) *Methods Enzymol. 115*, 157–171.

Kabsch, W. (1988a) *J. Appl. Crystallogr. 21*, 67–71.

Kabsch, W. (1988b) *J. Appl. Crystallogr. 21*, 916–924.

Kennard, O., Isaacs, N. W., Motherwell, W. D. S., Coppola, J. C., Wampler, D. L., Larson, A. C., & Watson, D. G. (1971) *Proc. R. Soc. London, Ser. A 325*, 401.

Koyama, G., Iitaka, Y., Maeda, K., & Umezawa, H. (1968) *Tetrahedron Lett.*, 1875.

Kraulis, P. J. (1991) *J. Appl. Crystallogr. 24*, 946–950.

Lee, B., & Richards, F. M. (1971) *J. Mol. Biol. 55*, 379–400.

Le Goffic, F., Baca, B., Soussy, C. J., Dublanchet, A., & Duval, J. (1976a) *Ann. Microbiol. 127A*, 391–399.

Le Goffic, F., Martel, A., Capmau, M. L., Baca, B., Goebel, P., Chardon, H., Soussy, C. J., Duval, J., & Bouanchaud, D. H. (1976b) *Antimicrob. Agents Chemother. 10*, 258–264.

Liao, H. H. (1991) *Protein Expression Purif. 2*, 43–50.

Liao, H., McKenzie, T., & Hageman, R. (1986) *Proc. Natl. Acad. Sci. U.S.A. 83*, 576–580.

Moellering, R. C., Jr. (1983) *Rev. Infect. Dis. 5*, S212–S232.

Morrison, J. F., & Cleland, W. W. (1980) *Biochemistry 19*, 3127–3131.

Navaza, J. (1987) *Acta Crystallogr. A43*, 645–653.

Sadaie, Y., Burtis, K. C., & Doi, R. H. (1980) *J. Bacteriol. 141*, 1178–1182.

Sakon, J., Liao, H. H., Kanikula, A. M., Benning, M. M., Rayment, I., & Holden, H. M. (1993) *Biochemistry 32*, 11977–11984.

Schwotzer, U., Kayser, F. H., & Schwotzer, W. (1978) *FEMS Microbiol. Lett. 3*, 29–33.

Shaw, K. J., Rather, P. N., Hare, R. S., & Miller, G. H. (1993) *Microbiol. Rev. 57*, 138–163.

Studier, F. W., & Moffatt, B. A. (1986) *J. Mol. Biol. 189*, 113–130.

Tronrud, D. E., Ten Eyck, L. F., & Mathews, B. W. (1987) *Acta Crystallogr. A43*, 489–501.

Van Pelt, J. E., Iyengar, R., & Frey, P. (1986) *J. Biol. Chem. 261*, 15995–15999.

BI951464Q